

1-1-2024

Th2 and Th17-associated immunopathology following SARS-CoV-2 breakthrough infection in Spike-vaccinated ACE2-humanized mice

Tianyi Zhang
Louisiana State University

Nicholas Magazine
Louisiana State University

Michael C. McGee
Louisiana State University

Mariano Carossino
Louisiana State University

Gianluca Veggiani
Louisiana State University

See next page for additional authors

Follow this and additional works at: https://repository.lsu.edu/animalsciences_pubs

Recommended Citation

Zhang, T., Magazine, N., McGee, M., Carossino, M., Veggiani, G., Kousoulas, K., August, A., & Huang, W. (2024). Th2 and Th17-associated immunopathology following SARS-CoV-2 breakthrough infection in Spike-vaccinated ACE2-humanized mice. *Journal of Medical Virology*, 96 (1) <https://doi.org/10.1002/jmv.29408>


This Article is brought to you for free and open access by the School of Animal Sciences at LSU Scholarly Repository. It has been accepted for inclusion in Faculty Publications by an authorized administrator of LSU Scholarly Repository. For more information, please contact ir@lsu.edu.

Authors

Tianyi Zhang, Nicholas Magazine, Michael C. McGee, Mariano Carossino, Gianluca Veggiani, Konstantin G. Kousoulas, Avery August, and Weishan Huang

RESEARCH ARTICLE

Th2 and Th17-associated immunopathology following SARS-CoV-2 breakthrough infection in Spike-vaccinated ACE2-humanized mice

Tianyi Zhang¹ | Nicholas Magazine¹ | Michael C. McGee¹ | Mariano Carossino^{1,2} | Gianluca Veggiani¹ | Konstantin G. Kousoulas¹  | Avery August³ | Weishan Huang^{1,3}

¹Department of Pathobiological Sciences, Louisiana State University, Baton Rouge, Louisiana, USA

²Louisiana Animal Disease Diagnostic Laboratory, School of Veterinary Medicine, Louisiana State University, Baton Rouge, Louisiana, USA

³Department of Microbiology and Immunology, Cornell University, Ithaca, New York, USA

Correspondence

Weishan Huang, Department of Pathobiological Sciences, Louisiana State University, 1909 Skip Bertman Dr, Baton Rouge, LA 70803, USA.
Email: huang1@lsu.edu

Funding information

Louisiana State University; National Institutes of Health, Grant/Award Numbers: P20 GM130555-6610, P20 GM130555-5011, R01 AI151139

Abstract

Vaccines have demonstrated remarkable effectiveness in protecting against COVID-19; however, concerns regarding vaccine-associated enhanced respiratory diseases (VAERD) following breakthrough infections have emerged. Spike protein subunit vaccines for SARS-CoV-2 induce VAERD in hamsters, where aluminum adjuvants promote a Th2-biased immune response, leading to increased type 2 pulmonary inflammation in animals with breakthrough infections. To gain a deeper understanding of the potential risks and the underlying mechanisms of VAERD, we immunized ACE2-humanized mice with SARS-CoV-2 Spike protein adjuvanted with aluminum and CpG-ODN. Subsequently, we exposed them to increasing doses of SARS-CoV-2 to establish a breakthrough infection. The vaccine elicited robust neutralizing antibody responses, reduced viral titers, and enhanced host survival. However, following a breakthrough infection, vaccinated animals exhibited severe pulmonary immunopathology, characterized by a significant perivascular infiltration of eosinophils and CD4⁺ T cells, along with increased expression of Th2/Th17 cytokines. Intracellular flow cytometric analysis revealed a systemic Th17 inflammatory response, particularly pronounced in the lungs. Our data demonstrate that aluminum/CpG adjuvants induce strong antibody and Th1-associated immunity against COVID-19 but also prime a robust Th2/Th17 inflammatory response, which may contribute to the rapid onset of T cell-mediated pulmonary immunopathology following a breakthrough infection. These findings underscore the necessity for further research to unravel the complexities of VAERD in COVID-19 and to enhance vaccine formulations for broad protection and maximum safety.

KEYWORDS

breakthrough infection, eosinophil, pulmonary immunopathology, Spike protein vaccine, Th17, Th2

This is an open access article under the terms of the [Creative Commons Attribution-NonCommercial](https://creativecommons.org/licenses/by-nc/4.0/) License, which permits use, distribution and reproduction in any medium, provided the original work is properly cited and is not used for commercial purposes.

© 2024 The Authors. *Journal of Medical Virology* published by Wiley Periodicals LLC.

1 | INTRODUCTION

Coronavirus disease 2019 (COVID-19), which is caused by severe acute respiratory syndrome coronavirus 2 (SARS-CoV-2), has stimulated global efforts of vaccine development and administration. The SARS-CoV-2 Spike protein has been used as a primary vaccine antigen, given its dominant role in mediating SARS-associated coronavirus infection.¹ Spike-based vaccines are safe and effective in reducing severe COVID-19 (see Review²). However, protective immunity elicited by SARS-CoV-2 infection or COVID-19 vaccines may wane rapidly, leading to a rapid decrease in protective effectiveness within 6 months.^{3–5} In addition, due to the active evolution of SARS-CoV-2, new variants of concern can gain the ability to evade prior immunity, notably neutralizing antibodies, via selection against the immune epitopes.⁶ Under such circumstances, breakthrough infections in vaccinated individuals could occur fairly soon after vaccination,^{7,8} independent of demographic factors or comorbidities.⁹

Vaccine-associated enhanced respiratory diseases (VAERD) can occur in vaccinated individuals during breakthrough infections. It is well documented in humans that formalin-inactivated Respiratory Syncytial Virus (RSV) vaccines could cause lung eosinophilia, leading to enhanced respiratory diseases in infants and young children during breakthrough RSV infections.¹⁰ While VAERD has not been reported in humans following COVID-19 breakthrough infections, in animal models, SARS-associated coronavirus vaccines have been shown to enhance type 2 immunopathology (IL-4/5/13 and eosinophils) in the lung following breakthrough infections.^{11–13} This has been reported in multiple animal species including mice, hamsters, ferrets and nonhuman primates, and even more concerning, with multiple vaccine types including inactivated vaccine, virus-like particle vaccine containing multiple virus proteins, Spike-expressing viral vector vaccine, and Spike protein subunit vaccine.^{11–13} Although adjuvants are not required for the development of SARS-associated coronavirus VAERD in animals, aluminum-based (Alum) adjuvants can aggravate the observed vaccine-associated Th2-biased pulmonary immunopathology for Spike protein subunit vaccine.¹³ Alum-based adjuvants predominantly skew towards Th2 effector cell differentiation and a strong humoral immunity¹⁴; they are also the most widely used adjuvants in human vaccines.¹⁵ CpG oligodeoxynucleotides (CpG), a soluble Toll-like receptor 9 (TLR9) ligand, can increase both cellular and humoral immunity, particularly with strong Th1 and CD8⁺ T cell immunity.¹⁶ In aged BALB/c mice, the combination of Alum and CpG has been used in COVID-19 subunit vaccines containing Spike Receptor-Binding Domain (RBD) as antigen.^{17,18} Compared to Alum or CpG alone, the combination of both adjuvants enhanced host protection against a mouse-adapted SARS-CoV-2 strain.¹⁸ It is however unclear whether this combined adjuvant strategy is safe and effective in humans.

In this study, we investigated safety and efficacy of a Spike protein subunit vaccine adjuvanted with Alum and CpG in an ACE2-

humanized mouse model, along with the human isolate of SARS-CoV-2 (USA-WA1/2020). As expected, vaccination with Spike protein in combination with Alum + CpG adjuvant induced robust neutralizing antibody production, Th1 effector cells, and Spike-specific CD8⁺ T cells. However, in the face of breakthrough infections, despite a significant reduction of mortality and lung viral load, vaccinated mice suffered substantial pulmonary immunopathology. As previously reported, the observed lung pathology is associated with eosinophilia and enhanced Th2 effector immunity. To our surprise, we also observed a substantial systemic Th17 response, most prominently in the lung. Our results reveal the predominant Th17-associated inflammatory response in ACE2-humanized mice, following COVID-19 vaccination and breakthrough infection. This model may be used to investigate COVID-19 vaccine-associated enhanced respiratory diseases.

2 | MATERIALS AND METHODS

2.1 | Mice

B6. Cg-Tg(K18-ACE2)2Prlmn/J (K18-hACE2; Strain #:034860) mice were purchased from the Jackson Laboratory and housed in the Division of Laboratory Animal Medicine, at Louisiana State University School of Veterinary Medicine. All experiments were approved by the Institutional Animal Care and Use Committee at Louisiana State University.

2.2 | Immunization and SARS-CoV-2 infection

Male mice at the age of around 10 weeks were immunized intramuscularly (I.M., ipsilateral administration) in a prime-boost regimen (Figure 1, day 0 and day 21) with 5 µg/dose of recombinant SARS-CoV-2 Spike protein (S1 + S2 extracellular domain) (Bon Opus Biosciences, #BP040) adjuvanted with 100 µg/dose Alum (alhydrogel adjuvant 2%, InvivoGen, #vac-alu-250) and 20 µg/dose CpG (ODN 2395 - TLR9 ligand, InvivoGen, #tlrl-2395-5) in 100 µL of PBS (pH 7.4). Mice vaccinated with PBS were used as negative controls. Blood was collected from the facial vein at the indicated time points, before infection, to confirm the induction of Spike-specific antibodies, neutralizing antibodies, and total IgE. Control and vaccinated mice were initially challenged with a low dose (500 PFU) of SARS-CoV-2 (USA-WA1/2020, BEI Resources, # NR-52281), followed by a high dose (10 000 PFU) infection of the same virus 3 days later. Viruses were delivered to mice intranasally in 50 µL of sterile PBS. Infected animals were monitored daily. Mice that did not respond to back padding or lost ≥20% of original weight were humanely euthanized and recorded as a death event. Seven days post the initial infections (dpi), all viable animals were euthanized for analyses. Serum, spleen, lung and mediastinal lymph nodes were collected.

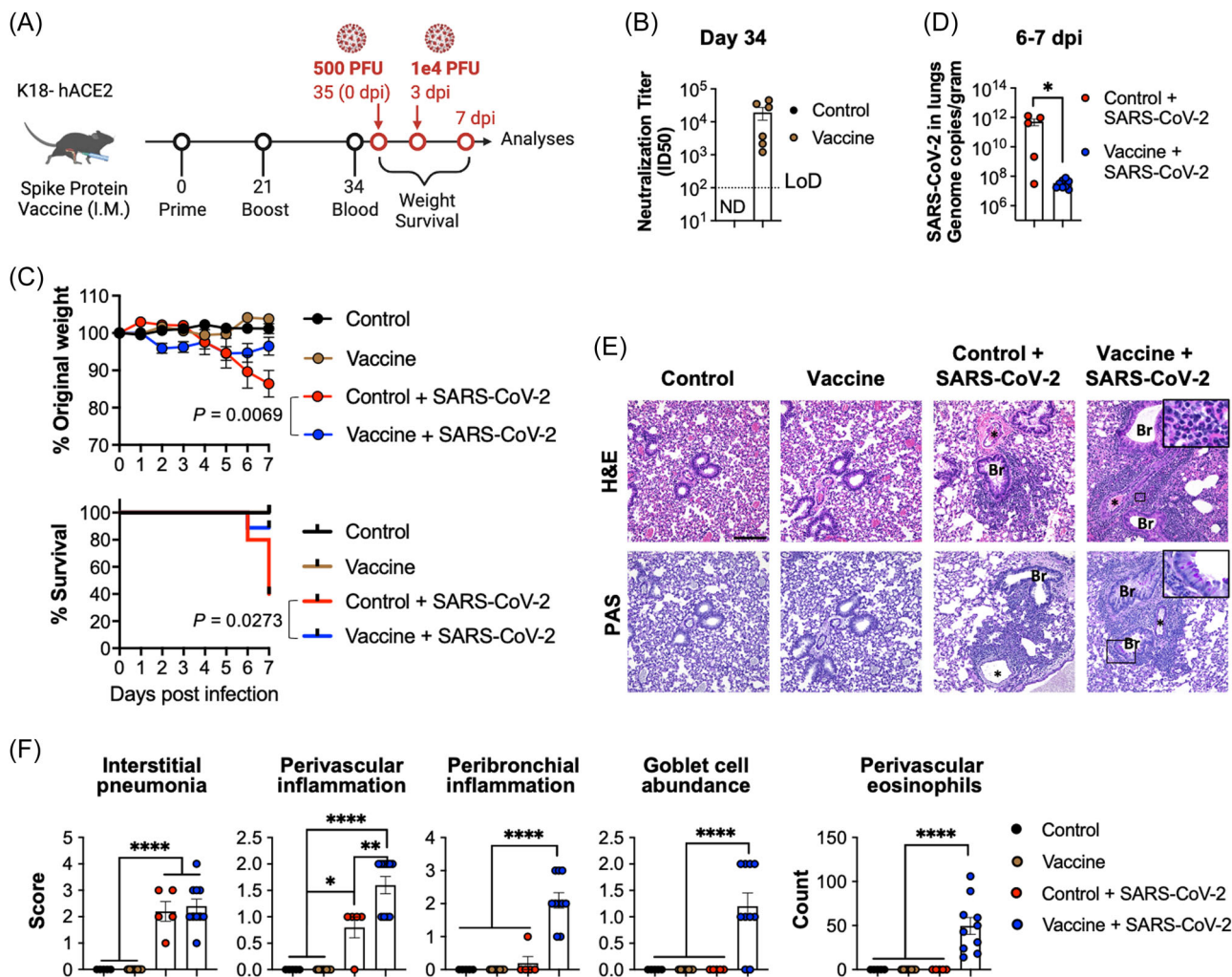


FIGURE 1 Protective effects and VAERD in hACE2 transgenic mice following SARS-CoV-2 Spike protein vaccination and breakthrough infection. (A) Schematic of experimental design. K18-hACE2 mice were vaccinated with PBS (Control) or SARS-CoV-2 Spike protein (Vaccine) intramuscularly (I.M.), followed by challenge with increasing dosage of SARS-CoV-2 administered intranasally (I.N.). (B) Neutralizing antibody titers following vaccination. Before infection (day 34 post vaccine priming), sera were collected from mice and analyzed in neutralization assays to verify the induction of neutralizing antibodies by vaccination (Control $n = 5$; Vaccine $n = 6$ randomly sampled from each cage). Limit of detection, LoD = 100. (C) Percentage of original body weight and survival at the indicated time points. P value in weight curve was calculated by two-way ANOVA. P value in survival curve was calculated by log-rank test. Animals that lost $\geq 20\%$ body weight were euthanized and recorded as dead, and organs were collected for analysis. All animals were euthanized at the beginning of day 7 post infection. (D) SARS-CoV-2 viral load (genome copies/gram) in lungs (Control + SARS-CoV-2 $n = 5$; Vaccine + SARS-CoV-2 $n = 10$). * $p \leq 0.05$ by two-tailed student's t test. (E) Representative images of H&E and PAS staining of lung tissue sections. Magnification: 200 \times . Scale bar = 100 μ m. Br denotes bronchioles and * denotes pulmonary vasculature. Rectangles indicate zoom-in areas depicting increase in perivascular eosinophils and higher frequency of goblet cells in the bronchiolar epithelium. (F) Histopathological scores. Control $n = 3$; Vaccine $n = 8$; Control + SARS-CoV-2 $n = 5$; Vaccine + SARS-CoV-2 $n = 10$. * $p < 0.05$, ** $p < 0.01$, **** $p < 0.0001$ by one-way ANOVA with multiple comparisons. Data presented as Mean \pm S.E.M.

2.3 | Serum neutralizing antibody titration

Calu-3 cells (ATCC; HTB-55) (1×10^5 /well in 50 μ l) were seeded in 96-well plates, followed by incubation in 37°C, with 5% CO₂, for 6–12 h before infection. Titrated sera were mixed with SARS-CoV-2 virus (US-AWA1/2020; 1000 PFU) in 50 μ l and incubated in 37°C for 30 min, and then applied to the seeded cells. Forty hours post infection, supernatant was removed, and cells were incubated with 60 μ l of 0.25% trypsin-EDTA (25200072; ThermoFisher Scientific) for 2–3 min, followed by the addition of 120 μ l of 6% paraformaldehyde (PFA)/PBS. Cells were then

transferred to V-bottom plates and fixed overnight. Fixed cells were then permeabilized and stained (using BioLegend Buffer 421002) for intracellular SARS-CoV-2 nucleocapsid (N) protein using a monoclonal Alexa Fluor 647-conjugated anti-N antibody (kind gift from Dr. Yongjun Guan). Flow cytometric data were acquired with an automatic plate reader system (CytoFlex, Beckman Coulter, Inc.), and analyzed using FlowJo Software (version 10.1, FlowJo, LLC). Percentages of infection and dilution factors were used for nonlinear regression to calculate for doses for 50% inhibition (ID50) indicated by the dilution factors in Prism 9.3.1 (GraphPad).

2.4 | Quantitative reverse-transcription PCR (qRT-PCR)

The post-caval lobe of the lung was weighed and homogenized in 1 ml of PBS (pH 7.4) using a TissueLyser LT (Qiagen). RNA was extracted using TRIzol™ LS Reagent (Invitrogen) and cDNA was generated using Protoscript II First Strand cDNA Synthesis Kit (New England Biolabs). SARS-CoV-2 was detected by PCR using the 2019-nCoV RUO Kit (IDT DNA, # 10006713). To quantify viral genome copies, quantitative PCR (qPCR) Extraction Control from Heat-Inactivated SARS-Related Coronavirus 2, Isolate USA-WA1/2020 (BEI Resources, # NR-52347) was used to generate the standard curve, which was used for calculating the genome copies per gram in the lung samples. To quantify cytokine gene transcript levels, “Best Coverage” gene probes for mouse Gapdh (Mm99999915_g1), Ifng (Mm01168134_m1), Il4 (Mm00445259_m1), Il13 (Mm00434204_m1), Il17a (Mm00439618_m1), Il21 (Mm00517640_m1), Gmcsf (Mm01290062_m1), and Il10 (Mm01288386_m1) (Applied Biosystems TaqMan Assays) were used as per manufacturer's instructions. Relative mRNA expression levels were calculated by normalizing cytokine gene values to the internal loading control Gapdh, and then further normalized against the average of cytokine levels in the control (unimmunized, uninfected).

2.5 | Histopathology and immunohistochemistry

Sections of the lung were fixed in 10% neutral buffered formalin for a minimum of 72 h and subsequently processed and embedded in paraffin following standard procedures. Serial four-micron tissue sections were either stained with hematoxylin and eosin (H&E) or subjected to the Periodic acid Schiff reaction (PAS) following standard procedures.

For mouse CD4 immunohistochemistry, sections were mounted on positively charged Superfrost Plus slides (Fisher Scientific) and processed using the automated BOND-RXm system (Leica Biosystems). Following automated deparaffinization, tissue sections were subjected to automated heat-induced epitope retrieval using a ready-to-use EDTA-based solution (pH 9.0; Leica Biosystems) for 20 min at 100°C. Subsequently, endogenous peroxidase was quenched by incubation with 3% hydrogen peroxide for 5 min, followed by incubation with a recombinant rabbit anti-mouse CD4 monoclonal antibody (clone EPR19514; Abcam) diluted 1:4,000 in a ready-to-use antibody diluent (Leica Biosystems) for 30 min at room temperature. Sections were then washed and stained with a polymer-labeled goat anti-rabbit IgG conjugated to HRP for 8 min, followed by incubation with HRP substrate for 10 min, at room temperature. Counterstaining was performed with hematoxylin for 5 min and slides were finally mounted with Micromount (Leica Biosystems).

Scoring of stained tissue sections was based on a cumulative score (maximum attainable score of 17) derived from five specific

histologic features evaluated in five random 20× fields following the scoring rubrics shown in Supplemental Table S1. Additionally, absolute eosinophil counts within perivascular cuffs were performed in 3 randomly selected perivascular cuffs.

2.6 | Flow cytometric analyses

For flow cytometric analyses, spleens, mediastinal lymph nodes, and lungs were homogenized via grinding against strainers, followed by filtering through the strainers. Red blood cells were lysed with RBC Lysis Buffer (Tonbo Biosciences, #TNB-4300-L100), followed by washing and pelleting. Cells were resuspended in full RPMI-1640 media for counting, staining and analysis via flow cytometry. Surface protein staining was performed with antibodies for surface markers in PBS pH 7.4, in the presence of Fc Block (TruStain FcX™, BioLegend, # 101319) and fixable viability dye (Ghost Dye™ Violet 510, Tonbo Biosciences) at room temperature for 30 min. To measure cytokine production after *ex vivo* stimulation, 500 µl single-cell suspensions were incubated at 37°C for 6 h with 5% CO₂ in 48-well plates in the presence of Cell Stimulation Cocktail (Tonbo Biosciences, #TNB-4975). Stimulated cells were stained with surface markers as described above, then were fixed with 4% PFA (diluted by PBS) at 4°C overnight, followed by permeabilization and staining using the eBioscience Intracellular Permeabilization Buffer (Invitrogen, #88-8824-00). Flow data were acquired using the LSRFortessa X-20 cell analyzer (BD Biosciences) and analyzed using FlowJo. The list of antibodies used is available in Supplemental Materials.

2.7 | Statistical analysis

T-test, one-way ANOVA and two-way ANOVA results with $p \leq 0.05$ were considered statistically significant. Survival rates were compared by log-rank test, with $p \leq 0.05$ considered as significantly different. All the statistical tests were performed using GraphPad Prism version 9.3.1 (GraphPad, San Diego, CA).

3 | RESULTS

3.1 | Protective effects of Spike vaccination in breakthrough infection in ACE2-humanized mice

To further investigate the protective and immunopathogenic effects of vaccine-induced host immunity in COVID-19 vaccination in a humanized animal model, we immunized K18-hACE2 mice intramuscularly with a prime-boost regimen with 5 µg per dose of SARS-CoV-2 Spike protein mixed with Alum and CpG adjuvants (Figure 1A). Following vaccination, to simulate breakthrough infection, we infected animals with increasing dosages of virus (Figure 1A). This

protocol was chosen to allow a prolonged stimulation on T cells following live viral infection, while retaining a high survival rate of the control (unvaccinated) group for analyses at day 7 post SARS-CoV-2 infection. ELISA and neutralization assays on post-vaccination but pre-exposure sera verified that our SARS-CoV-2 Spike protein vaccination induced high levels of Spike-specific IgG (see Figure S1A) and high titers of neutralizing antibodies (Figure 1B). In mouse models of vaccination, IgG1 production is more associated with a Th2-like response to immunization, while IgG2a/IgG2c production is strongly correlated with Th1-associated immunity.^{19–21} We observed similar endpoint titers of Spike-specific IgG1 and IgG2c in the vaccinated animals, suggesting that both Th1 and Th2-associated immune responses were elicited following vaccination of Spike protein in the presence of Alum and CpG (Figure S1B). Spike-protein vaccination provided protection by preventing severe morbidity and mortality (Figure 1C). Notably, while the vaccination protected against the infection by reducing the overall viral loads in the lungs, the two-dose virus exposure allowed the establishment of a breakthrough infection in the vaccinated animals ($\sim 10^{12}$ vs. $\sim 10^8$ genome copies/gram lung tissue, comparing unvaccinated vs. vaccinated animals) (Figure 1D).

3.2 | Type 2 pulmonary immunopathology following Spike vaccination and breakthrough infection

Despite a significantly improved survival rate, vaccinated animals appeared distressed assuming a hunched posture, exhibiting reluctance to move and lethargy. Histological staining of the lung sections revealed that the breakthrough infections caused a significant level of interstitial pneumonia comparable to that observed in the unvaccinated and infected mice (Figure 1E,F). Moreover, breakthrough infections in vaccinated animals resulted in elevated levels of perivascular and peribronchial inflammation, as compared to the lungs of the unvaccinated and infected mice (Figure 1E,F). The observed severe immunopathology in vaccinated mice following breakthrough infections was associated with significant increase in the abundance of goblet cells and increased counts of perivascular eosinophils (Figure 1E,F). Flow cytometric analyses of cells recovered from the lungs further revealed significant accumulation of eosinophils and IgE-bound basophils/mast cells in the vaccinated mice with breakthrough infections (Figure 2A, B). We also noticed that, before infection, vaccination with Spike protein in Alum and CpG adjuvants was sufficient in inducing high levels of IgE production detected in the sera collected 7 days post the vaccine boost (Figure S1C). Also, we detected a trend of higher levels of Spike-specific IgE production in the vaccinated mice (Figure S1C). On the other hand, the increased numbers of interstitial macrophages and dendritic cells in the lungs following SARS-CoV-2 infection were not affected by vaccination, while

the infection-driven neutrophil enrichment in the lung was significantly reduced by vaccination, though not to levels comparable to those observed in uninfected mice (Figure 2B). In agreement with previous findings,¹³ our results show that immunization with Spike protein followed by a breakthrough SARS-CoV-2 infection causes a type 2-associate inflammatory response, prominently eosinophilia in the lung, which leads to vaccine-associated respiratory pathology in animal models of COVID-19.

3.3 | Massive lung infiltration of CD4⁺ T cells following Spike protein vaccination and breakthrough infection

We investigated the effects of Spike vaccination on lymphocytes in the lungs of the mice with breakthrough infections by flow cytometric analyses (Figure 3A). In the absence of an infection, immunization with Spike protein did not cause lymphocyte enrichment in the lungs (Figure 3B). However, following infection, the numbers of NK cells, invariant NKT cells, and CD8⁺ T cells in the lungs substantially increased, with no significant differences between unvaccinated and vaccinated animals (Figure 3B). In contrast, we observed significantly increased lung infiltration of B cells, $\gamma\delta$ T cells and CD4⁺ T cells in the vaccinated and infected animals (Figure 3B), with the lung-infiltrating CD4⁺ T cells representing the most abundant lymphocyte population in the vaccinated animals with a breakthrough infection (Figure 3B). To further determine the histological locations of CD4⁺ T cell infiltration, we subjected lung tissue sections to immuno-histochemical analysis, and observed CD4⁺ T cells throughout the lung tissue sections with a perivascular enrichment (Figure 3C). These data suggest that these CD4⁺ T cells might be recruited to the lungs during breakthrough infection.

3.4 | Th2 and Th17-associated pulmonary inflammatory cytokine responses following Spike vaccination and breakthrough infection

Given the type 2-associated pulmonary immunopathology and the massive CD4⁺ T cell infiltration in the lungs of ACE2-humanized animals following Spike immunization and breakthrough infection (Figures 1–3), we suspected that there was an enhanced Th2 cytokine response involved. To further compare the levels of other T helper subtype-associated cytokine production, we quantified the levels of gene expression of cytokines associated with different T helper cell subtypes,^{22,23} including *Ifng* (Th1), *Il4/Il13* (Th2), *Il17a* (Th17), *Il21* (Tfh), *Csf2* (encodes GM-CSF), and *Il10* (Regulatory T cells) (Figure 4). We found that SARS-CoV-2 infection induced high levels of expression of *Ifng* in both unvaccinated and vaccinated mice, and as expected, vaccination with Spike protein followed by a

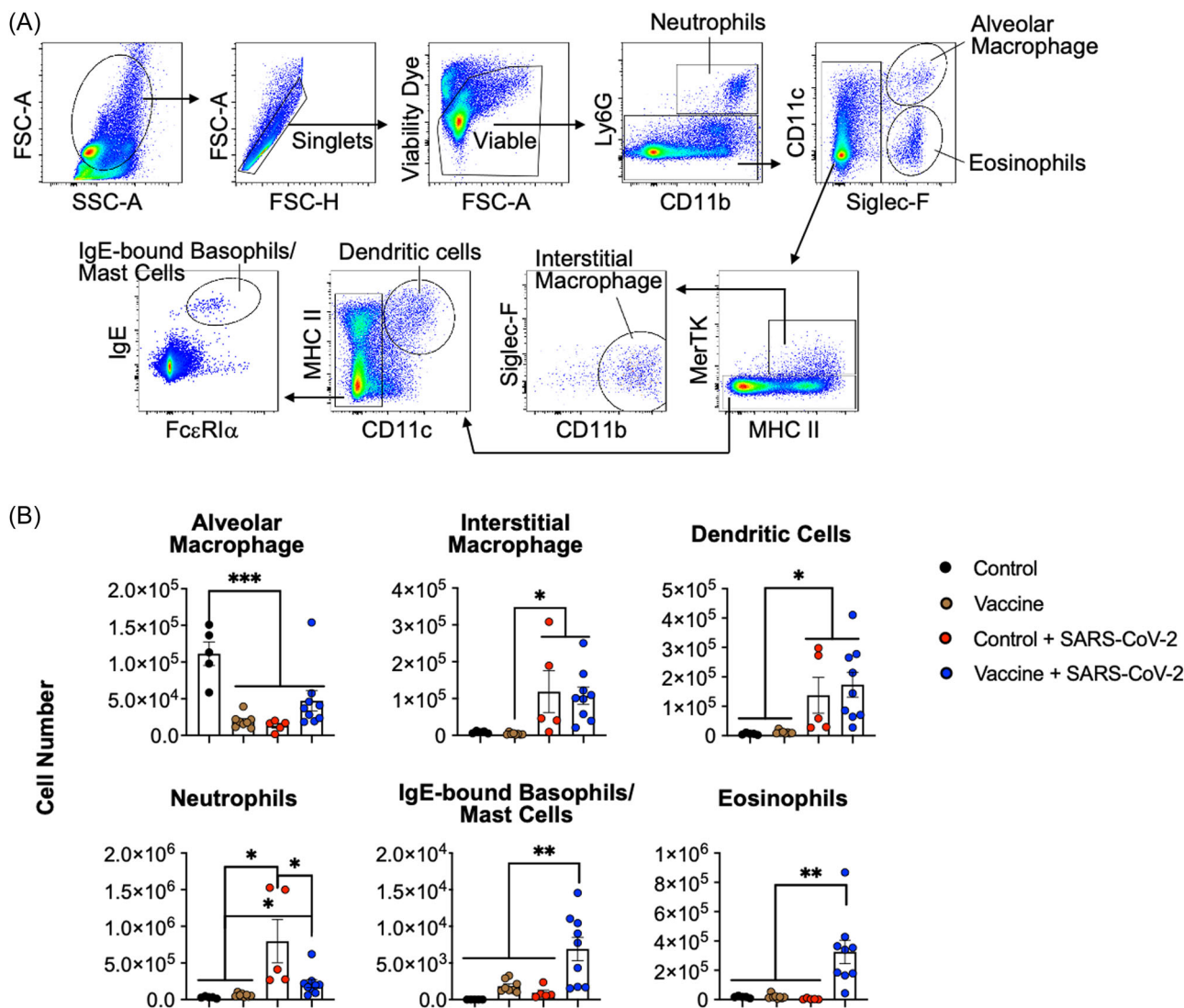


FIGURE 2 Pulmonary innate immune cell profile. (A) Representative flow cytometric plots for innate immune cell gating. Cells were stained and fixed overnight before analyses. (B) Numbers of the indicated innate immune cells in the lungs. Control $n = 5$; Vaccine $n = 8$; Control + SARS-CoV-2 $n = 5$; Vaccine + SARS-CoV-2 $n = 9$. * $p < 0.05$, ** $p < 0.01$, *** $p < 0.001$ by one-way ANOVA with multiple comparisons. Data presented as Mean \pm S.E.M.

breakthrough infection led to elevated expression of Th2 cytokines *Il4* and *Il13*. Similarly, the expression of *Il21* was significantly higher in the vaccinated and infected animals compared to untreated controls or mice that were vaccinated but not infected. There was a trend of increased expression of *Il21* in the vaccinated and infected group as compared to the unvaccinated and infected mice, suggesting a strong Tfh cell response in the vaccinated and infected animals. Vaccination showed an inhibitory effect on virus-associated induction of the expression of *Il10* and *Csf2*. To our surprise, the expression of *Il17a* was significantly higher in the vaccinated and infected animals, as compared to any other groups, suggesting that a Th17-associated inflammatory response was likely involved in the development of the VAERD observed in the Spike-vaccinated mice that suffer a breakthrough infection (Figure 4).

3.5 | A systemic Th17 inflammatory response following Spike vaccination and breakthrough infection

We suspected that the CD4⁺ T cell population was responsible for the elevated *Il17a* expression, given that they were the most abundant infiltrating lymphocytes in the lungs of animals with severe VAERD. To confirm this hypothesis, we stimulated cells recovered from the lung, draining lymph node of the vaccinated site, and the spleen with a cell stimulation cocktail (containing PMA, ionomycin, and Brefeldin A), and performed intracellular cytokine staining for Th1 effector-associated cytokines (IFN- γ and TNF- α), Th2-associated cytokine (IL-4), and Th17 cytokine (IL-17A). We found that the percentage of cells expressing Th1, Th2 or Th17

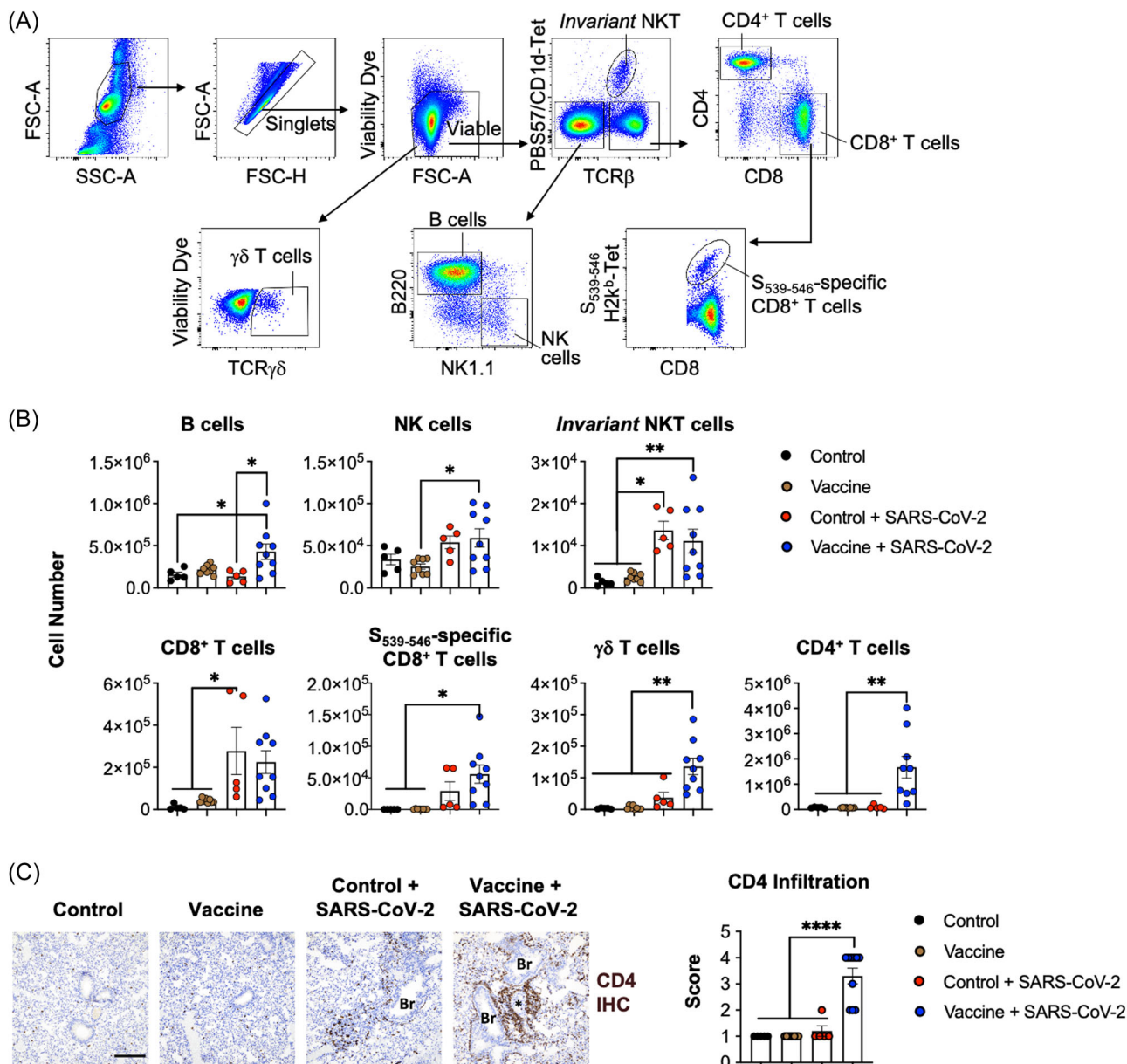


FIGURE 3 Pulmonary lymphocyte profile. (A) Representative flow cytometric plots for lymphocyte gating. Cells were stained and fixed overnight before analyses. (B) Numbers of the indicated lymphocytes in the lungs. (C) Representative immunohistochemical staining of CD4 (brown) and scores of CD4⁺ T cell infiltration in lung tissue sections. Magnification: 200 \times . Scale bar = 100 μ m. Br denotes bronchioles and *denotes pulmonary vasculature. Control $n = 5$; Vaccine $n = 8$; Control + SARS-CoV-2 $n = 5$; Vaccine + SARS-CoV-2 $n = 9$. * $p < 0.05$, ** $p < 0.01$, *** $p < 0.001$ by one-way ANOVA with multiple comparisons. Data presented as Mean \pm S.E.M.

cytokines were all significantly higher in the lungs and draining lymph nodes of the vaccinated and infected group compared to mice under any of the other conditions (Figure 5A,B). Strikingly, the increase of Th17 cell numbers in the vaccinated and infected animals appeared to be systemic, as it was highly significant in cells recovered from the spleen of the mice with VAERD (Figure 5A,B, Spleen panels). Note that the number of $\gamma\delta$ T cells was also significantly elevated in the vaccinated and infected mice compared to all other groups (Figure 3B). Considering that $\gamma\delta$ T cells are

capable producers of IL-17 which can initiate a Th17 inflammatory response,²⁴ we analyzed the production of different Th cell-associated cytokines in lung $\gamma\delta$ T cells as well. However, we did not find evidence of VAERD-associated patterns of cytokine production by the $\gamma\delta$ T cells (Figure S2). Our results suggested that the COVID-19 VAERD observed in the ACE2-humanized mouse model is associated with enhanced local Th1, Th2 and Th17 inflammatory responses, as well as systemic Th17-associated inflammation.

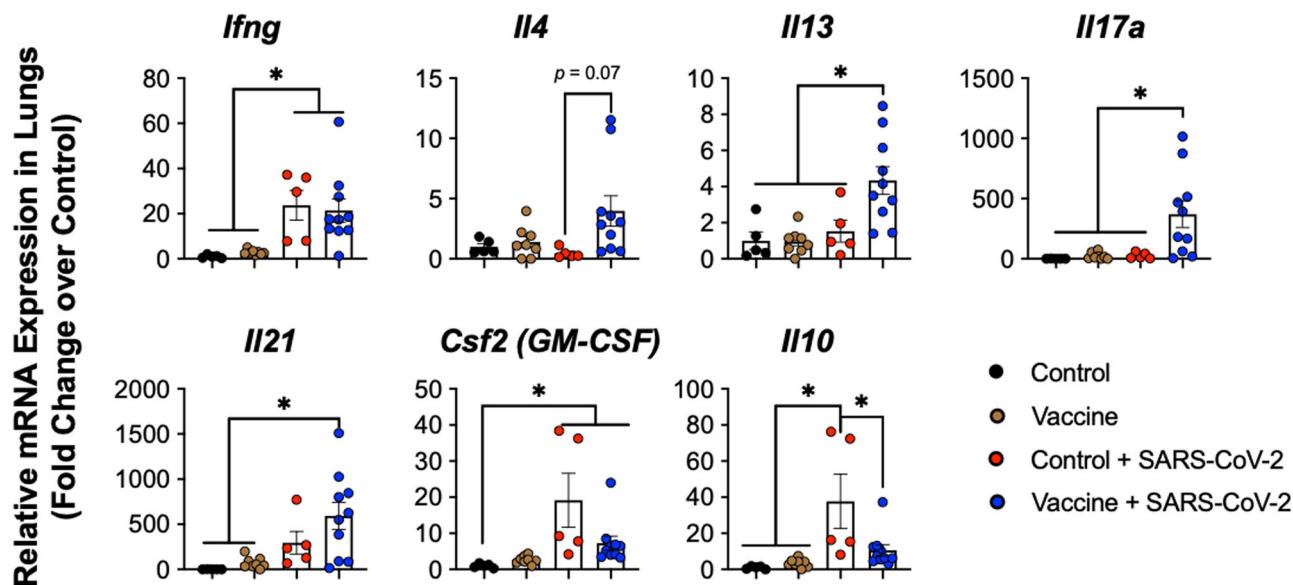


FIGURE 4 Pulmonary cytokine transcript production. Relative fold change in the expression of mRNAs encoding IL-4, IL-5, or IL-13 was determined using quantitative RT-PCR. After normalization to *Gapdh* expression, fold changes were calculated by normalization to the averages in the Control group. Control $n = 5$; Vaccine $n = 8$; Control + SARS-CoV-2 $n = 5$; Vaccine + SARS-CoV-2 $n = 10$. * $p < 0.05$ by one-way ANOVA with multiple comparisons. Data presented as Mean \pm S.E.M.

4 | DISCUSSION

It is undeniable that SARS-CoV-2 Spike-based vaccination is safe and effective in preventing severe and fatal COVID-19. Immunization against Spike protein using mRNA, viral vector-based or protein subunit vaccines can elicit protective immunity and prevent severe COVID-19 illness.²⁵ Our results further support the global consensus on the protective effects of vaccines. However, while COVID-19 vaccines have been successful in reducing the severity of the disease, additional efforts are needed to enhance our understanding of the complex dynamics of COVID-19 vaccination and the potential risks associated with breakthrough infections, especially concerning the emergence of VAERD. Multiple studies in different animal models of SARS-associated coronavirus infections reported that VAERD is associated with a Th2-biased inflammatory response.^{11–13} Here we systematically investigated the potential risks and underlying mechanisms of immunopathogenesis of VAERD in COVID-19 breakthrough infections. Using an ACE2-humanized mouse model of COVID-19, we observed a similar Th2-associated lung immunopathology following Spike immunization and SARS-CoV-2 breakthrough infection. Furthermore, our results suggest a prominent role of Th17 inflammatory response in correlation with severe COVID-19 VAERD. To the best of our knowledge, this is the first report of a prominent Th17 inflammatory response in VAERD in animal models of SARS-associated coronavirus infections.

In animal models, prior research on SARS-CoV-1 and SARS-CoV-2 vaccines suggested that VAERD may occur independently of the type of vaccines and/or adjuvants used.^{11–13} Although adjuvants are not required for the development of SARS-associated coronavirus VAERD in animals, Alum can aggravate Th2-biased pulmonary

immunopathology for Spike protein subunit vaccine.¹³ Alum-based adjuvant has been shown to help absorb and stabilize vaccine antigens and induce robust Th2-associated immunity and antibody production.^{26,27} Alum is the most used adjuvant in approved human vaccines,²⁸ including SARS-CoV-2 inactivated vaccines.^{29,30} Although no human cases of COVID-19 VAERD have been documented, in animal models including mouse, hamster, ferret, and nonhuman primates, SARS-associated VAERD has been reported, and Alum-associated Th2-biased pulmonary inflammation is considered a likely cause of VAERD.^{11–13} Recent research has focused on the development of novel vaccine adjuvants, and one of the key strategies is to enhance Alum-associated adjuvant effect by combining Alum with other adjuvants such as CpG, emulsive or particulate, to elicit and enhance both humoral and cellular immunity.^{31,32} Most studies analyze predominantly antiviral effects including neutralizing antibody titers, memory B cells, and antigen-specific effector T cells, following vaccination. VAERD is lesser a focus during vaccine development. It is critical to include analyses of VAERD in standard evaluations of vaccine safety.

The underlying molecular and cellular mechanisms of VAERD is unclear, despite the widely agreeable engagement of Th2-biased cellular immunity. Moreover, the duration and possibility of recurrence of VAERD have not been investigated. It is unclear whether the development and function of other effector and memory T cell responses such as Th1 and Th17, and regulatory T cells, are involved in the development and/or resolution of VAERD.

An increased production of Th1-associated cytokines (e.g., IFN- γ) is correlated with reduction in COVID-19 severity,³³ and vaccine-induced Th1 cell responses correlate with the protective effects of the current mRNA vaccines.³⁴ CpG ODNs that can stimulate TLR9

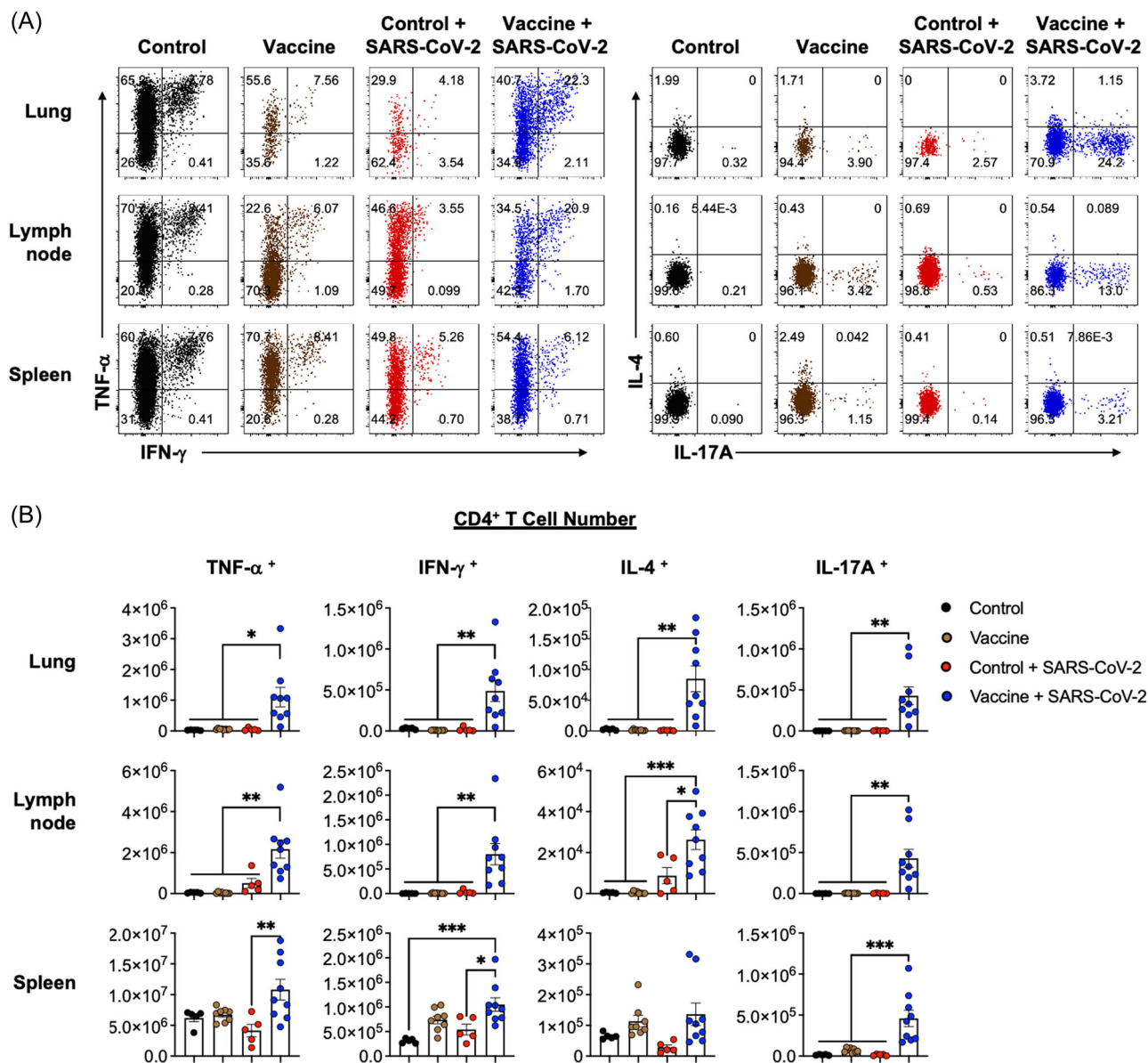


FIGURE 5 Effector cytokine production by CD4⁺ T cells. (A) Representative flow cytometric plots of TNF- α , IFN- γ , IL-4 and IL-17A expression by viable CD4⁺ T cells in lung, lymph node and spleen. (B) Numbers of CD4⁺ T cells in lung, lymph node and spleen expressing TNF- α , IFN- γ , IL-4 and IL-17A. Control $n = 5$; Vaccine $n = 8$; Control + SARS-CoV-2 $n = 5$; Vaccine + SARS-CoV-2 $n = 9$. * $p < 0.05$ by one-way ANOVA with multiple comparisons. Data presented as Mean \pm S.E.M.

and trigger strong Th1 type immunity have been considered as adjuvants for vaccinations against viral and bacterial infections, as well as cancer.¹⁶ Classic Alum adjuvants are the first licensed and most widely used vaccine adjuvants. Alum adjuvants can prime a Th2-biased T cell differentiation and promote humoral responses which provide effective protective immunity against many pathogens.¹⁴ However, in severe coronavirus diseases in humans, Th2 cytokine polarization has been associated with disease severity and increased mortality.³⁵ Additionally, Th2-skewing vaccination has consistently been linked to type 2 inflammatory immunity, notably eosinophilia, in cases of VAERD in animal models of coronaviral diseases.^{11–13,36,37} In mouse models of allergic airway inflammation,

where ovalbumin (OVA) is used to sensitize mice towards airway hypersensitivity upon respiratory exposure to OVA, Alum has been shown to induce a Th2-biased immunity accompanied by the induction of IgE and eosinophils. Interestingly, the effects of Alum in the OVA model could be reverted to basal levels by coadministration of CpG.³⁸ Similarly, the inclusion of Th1-skewing adjuvants in SARS-CoV-1 inactivated or Spike protein subunit vaccines attenuated the eosinophilic respiratory inflammatory responses during infections.^{39,40} Surprisingly, in SARS-CoV-2 Spike immunization followed by breakthrough infections, we observed elevated levels of lung immunopathology, eosinophilia, IgE, and Th2 responses, even if CpG and Alum were both used in vaccination. Moreover, we

observed a systemic Th17 pro-inflammatory response. This could be due to the intrinsic antigenic properties of the SARS-CoV-2 Spike protein. For example, the lethal Th2-associated immunopathology following SARS-CoV-1 Spike immunization and viral infection can be induced by certain regions of the SARS-CoV-1 Spike protein such as S₅₉₇₋₆₀₃ (LYQDVNC, an epitope downstream of the C terminus of the RBD),¹² which is identical to SARS-CoV-2 S₆₁₁₋₆₁₇.⁴¹ Since antibodies to this peptide have been shown to cause antibody-dependent enhancement (ADE) of infection in SARS-CoV-1, it is possible that SARS-CoV-2 S₆₁₁₋₆₁₇ may be involved in vaccine-associated enhanced pathology during infections through type 2 inflammation and potentially ADE.⁴¹ Similarly, other regions in SARS-CoV-2 Spike protein may be associated with a Th17 cell priming under the Alum/CpG combined adjuvant condition.

The induction of a systemic Th17 inflammatory response during breakthrough SARS-CoV-2 infection is particularly concerning. IL-17 exhibits multifaceted functions during viral infections. For example, during influenza infection, on one hand IL-17 promotes antiviral immunity and protects the hosts from severe viral disease, while on the other hand it contributes to the pathogenesis of immunopathology, lung injury, and post influenza superinfection.⁴² While the potential protective role of IL-17 in COVID-19 is unclear, there are documented associations between high IL-17 levels and COVID-19 pathogenesis. In severe COVID-19 patients, there are elevated levels of serum IL-17A and circulating Th17 cells.^{43,44} High serum levels of IL-17 were also observed in long-COVID.⁴⁵ IL-17 can not only cause skin and lung tissue inflammation and fibrosis,^{46,47} but also induces mucus production and goblet cell metaplasia in lung epithelial cells.^{48,49} IL-17 and neutrophils are also linked to thrombus formation in acute myocardial infarction.⁵⁰ Combined with TNF- α , IL-17A moderates thrombus growth on endothelial cells in vitro.⁵¹ In mouse models, IL-17A promotes deep vein thrombosis by enhancing platelet activation/aggregation, neutrophil infiltration, and endothelial cell activation.⁵² These features of Th17-associated inflammatory diseases should be considered in the analysis of potential COVID vaccine-associated adverse effects.

Another potential explanation of VAERD is dysregulation of regulatory immunity. Note that the level of IL-10 expression in the lungs of vaccinated and infected mice is significantly lower than that in unvaccinated but infected mice (Figure 4). Our knowledge of Treg cell development and function following COVID-19 vaccination and/or infection is limited, and the role of Treg cells in SARS-CoV-2 breakthrough infection in vaccinated individuals has not been reported. On the other hand, during acute respiratory viral infection such as influenza, Foxp3-negative T cells (type 1 regulatory T cells and CD8⁺ T cells) are major contributors to IL-10 production in the airway.⁵³ In the lungs of nonhuman primate models, IL-10 suppresses T cell expansion but promote tissue-resident memory T cell development during SARS-CoV-2 infection.⁵⁴ It is possible that Spike vaccination with Alum/CpG primes T cell differentiation in which IL-10-producing regulatory T cells are less favored. Future research may expand to investigate the role of IL-10 in counter-balancing pulmonary T cell expansion and memory development during COVID-19.

In conclusion, this research underscores the complexity of COVID-19 vaccination and the need for a comprehensive understanding of vaccine-induced immune responses. While vaccines remain a vital tool in combating pandemics, the potential for VAERD highlights the importance of ongoing research, surveillance, and careful vaccine development to achieve broad protection and maximal safety.

AUTHOR CONTRIBUTIONS

T.Z., N.M., M.C.M., M.C. and W.H. performed experiments and analyzed data; T.Z. and W.H. designed experiments and wrote the manuscript; W.H. secured funding and supervised the research; all authors reviewed, edited and finalized the manuscript.

ACKNOWLEDGMENTS

The SARS-CoV-2 USA-WA1/2020 strain and its quantitative PCR standard control were from the BEI Resources, while the CD1d and H2kb mouse tetramers were from the NIH Tetramer Core Facility. We also thank Dr. Yongjun Guan (previously at Antibody Biopharm Inc.) for his kind gift of the Alexa Fluor 647-labeled anti-SARS-CoV-2 N antibody, and members of the Huang and Veggiani groups for helpful discussions. This research was supported in part by grants from the National Institutes of Health (P20 GM130555-6610, P20 GM130555-5011 and R01 AI151139) and a Big Idea Research Grant from the Provost's Fund at Louisiana State University.

CONFLICTS OF INTEREST STATEMENT

W.H. receives research support from MegaRobo Technologies Co., Ltd. and A.A. receives sponsored program funding from 3M, which were not related to this study. The other authors claim no conflicts of interest.

DATA AVAILABILITY STATEMENT

The data that support the findings of this study are available upon reasonable request.

ORCID

Konstantin G. Kousoulas  <http://orcid.org/0000-0001-7077-9003>

REFERENCES

- Li W, Moore MJ, Vasilieva N, et al. Angiotensin-converting enzyme 2 is a functional receptor for the SARS coronavirus. *Nature*. 2003; 426(6965):450-454.
- Grana C, Ghosn L, Evrenoglou T, et al. Efficacy and safety of COVID-19 vaccines. *Cochrane Database Syst Rev*. 2022;12(12):CD015477.
- Hall V, Foulkes S, Insalata F, et al. Protection against SARS-CoV-2 after Covid-19 vaccination and previous infection. *N Engl J Med*. 2022;386(13):1207-1220.
- Levin EG, Lustig Y, Cohen C, et al. Waning immune humoral response to BNT162b2 Covid-19 vaccine over 6 months. *N Engl J Med*. 2021;385(24):e84.
- Choe PG, Kang CK, Suh HJ, et al. Waning antibody responses in asymptomatic and symptomatic SARS-CoV-2 infection. *Emerging Infect Dis*. 2021;27(1):327-329.
- Magazine N, Zhang T, Wu Y, McGee MC, Veggiani G, Huang W. Mutations and evolution of the SARS-CoV-2 Spike protein. *Viruses*. 2022;14(3):640.

7. Teran RA, Walblay KA, Shane EL, et al. Postvaccination SARS-CoV-2 infections among skilled nursing facility residents and staff members - Chicago, Illinois, December 2020-March 2021. *Am J Transplant (AJT)*. 2021;21(6):2290-2297.
8. Birhane M, Bressler S, Chang G, et al. COVID-19 vaccine breakthrough infections reported to CDC - United States, January 1-April 30, 2021. *MMWR Morb Mortal Wkly Rep*. 2021;70(21):792-793.
9. Butt AA, Yan P, Shaikh OS, Mayr FB. Outcomes among patients with breakthrough SARS-CoV-2 infection after vaccination in a high-risk national population. *EClinicalMedicine*. 2021;40:101117.
10. Kim HW, Canchola JG, Brandt CD, et al. Respiratory syncytial virus disease in infants despite prior administration of antigenic inactivated vaccine. *Am J Epidemiol*. 1969;89(4):422-434.
11. Bolles M, Deming D, Long K, et al. A double-inactivated severe acute respiratory syndrome coronavirus vaccine provides incomplete protection in mice and induces increased eosinophilic proinflammatory pulmonary response upon challenge. *J Virol*. 2011;85(23):12201-12215.
12. Tseng CT, Sbrana E, Iwata-Yoshikawa N, et al. Immunization with SARS coronavirus vaccines leads to pulmonary immunopathology on challenge with the SARS virus. *PLoS ONE*. 2012;7(4):e35421.
13. Ebenig A, Muraleedharan S, Kazmierski J, et al. Vaccine-associated enhanced respiratory pathology in COVID-19 hamsters after T(H)2-biased immunization. *Cell Rep*. 2022;40(7):111214.
14. Hogenesch H. Mechanism of immunopotentiality and safety of aluminum adjuvants. *Front Immunol*. 2012;3:406.
15. Verma SK, Mahajan P, Singh NK, et al. New-age vaccine adjuvants, their development, and future perspective. *Front Immunol*. 2023;14:1043109.
16. Bode C, Zhao G, Steinhagen F, Kinjo T, Klinman DM. CpG DNA as a vaccine adjuvant. *Expert Rev Vaccines*. 2011;10(4):499-511.
17. Pollet J, Strych U, Chen WH, et al. Receptor-binding domain recombinant protein on alum-CpG induces broad protection against SARS-CoV-2 variants of concern. *Vaccine*. 2022;40(26):3655-3663.
18. Nanishi E, Borriello F, O'Meara TR, et al. An aluminum hydroxide-CpG adjuvant enhances protection elicited by a SARS-CoV-2 receptor binding domain vaccine in aged mice. *Sci Transl Med*. 2022;14(629):eabj5305.
19. Germann T, Bongartz M, Dlugonska H, et al. Interleukin-12 profoundly up-regulates the synthesis of antigen-specific complement-fixing IgG2a, IgG2b and IgG3 antibody subclasses in vivo. *Eur J Immunol*. 1995;25(3):823-829.
20. Lefebvre DJ, Benaissa-Trouw B, Vliegthart JFG, et al. Th1-directing adjuvants increase the immunogenicity of oligosaccharide-protein conjugate vaccines related to *Streptococcus pneumoniae* type 3. *Infect Immun*. 2003;71(12):6915-6920.
21. Wang Y, Wang L, Cao H, Liu C. SARS-CoV-2 S1 is superior to the RBD as a COVID-19 subunit vaccine antigen. *J Med Virol*. 2021;93(2):892-898.
22. O'Shea JJ, Paul WE. Mechanisms underlying lineage commitment and plasticity of helper CD4+ T cells. *Science*. 2010;327(5969):1098-1102.
23. Herndler-Brandstetter D, Flavell RA. Producing GM-CSF: a unique T helper subset? *Cell Res*. 2014;24(12):1379-1380.
24. Martin B, Hirota K, Cua DJ, Stockinger B, Veldhoen M. Interleukin-17-Producing $\gamma\delta$ T cells selectively expand in response to pathogen products and environmental signals. *Immunity*. 2009;31(2):321-330.
25. Zhang Z, Mateus J, Coelho CH, et al. Humoral and cellular immune memory to four COVID-19 vaccines. *Cell*. 2022;185(14):2434-2451.e17.
26. Marrack P, McKee AS, Munks MW. Towards an understanding of the adjuvant action of aluminium. *Nat Rev Immunol*. 2009;9(4):287-293.
27. Lee S, Nguyen MT. Recent advances of vaccine adjuvants for infectious diseases. *Immune Netw*. 2015;15(2):51-57.
28. Laera D, Hogenesch H, O'Hagan DT. Aluminum adjuvants-back to the future. *Pharmaceutics*. 2023;15(7):1884.
29. Xia S, Zhang Y, Wang Y, et al. Safety and immunogenicity of an inactivated SARS-CoV-2 vaccine, BBIBP-CorV: a randomised, double-blind, placebo-controlled, phase 1/2 trial. *Lancet Infect Dis*. 2021;21(1):39-51.
30. Zhang Y, Zeng G, Pan H, et al. Safety, tolerability, and immunogenicity of an inactivated SARS-CoV-2 vaccine in healthy adults aged 18-59 years: a randomised, double-blind, placebo-controlled, phase 1/2 clinical trial. *Lancet Infect Dis*. 2021;21(2):181-192.
31. Arunachalam PS, Walls AC, Golden N, et al. Adjuvanting a subunit COVID-19 vaccine to induce protective immunity. *Nature*. 2021;594(7862):253-258.
32. Pulendran B, S. Arunachalam P, O'Hagan DT. Emerging concepts in the science of vaccine adjuvants. *Nat Rev Drug Discovery*. 2021;20(6):454-475.
33. Jeyanathan M, Afkhami S, Smaill F, Miller MS, Lichty BD, Xing Z. Immunological considerations for COVID-19 vaccine strategies. *Nat Rev Immunol*. 2020;20(10):615-632.
34. Sahin U, Muik A, Derhovanessian E, et al. COVID-19 vaccine BNT162b1 elicits human antibody and T(H)1 T cell responses. *Nature*. 2020;586(7830):594-599.
35. Li CK, Wu H, Yan H, et al. T cell responses to whole SARS coronavirus in humans. *J Immunol*. 2008;181(8):5490-5500.
36. Iwata-Yoshikawa N, Shiwa N, Sekizuka T, et al. A lethal mouse model for evaluating vaccine-associated enhanced respiratory disease during SARS-CoV-2 infection. *Sci Adv*. 2022;8(1):eab3827.
37. Lindsley AW, Schwartz JT, Rothenberg ME. Eosinophil responses during COVID-19 infections and coronavirus vaccination. *J Allergy Clin Immunol*. 2020;146(1):1-7.
38. Mirotti LC, Alberca Custódio RW, Gomes E, et al. CpG-ODN shapes alum adjuvant activity signaling via MyD88 and IL-10. *Front Immunol*. 2017;8:47.
39. Iwata-Yoshikawa N, Uda A, Suzuki T, et al. Effects of toll-like receptor stimulation on eosinophilic infiltration in lungs of BALB/c mice immunized with UV-inactivated severe acute respiratory syndrome-related coronavirus vaccine. *J Virol*. 2014;88(15):8597-8614.
40. Honda-Okubo Y, Barnard D, Ong CH, Peng BH, Tseng CTK, Petrovsky N. Severe acute respiratory syndrome-associated coronavirus vaccines formulated with delta inulin adjuvants provide enhanced protection while ameliorating lung eosinophilic immunopathology. *J Virol*. 2015;89(6):2995-3007.
41. Zaichuk TA, Nechipurenko YD, Adzhubey AA, et al. The challenges of vaccine development against betacoronaviruses: antibody dependent enhancement and Sendai virus as a possible vaccine vector. *Mol Biol*. 2020;54(6):812-826.
42. Sahu U, Biswas D, Prajapati VK, Singh AK, Samant M, Khare P. Interleukin-17-A multifaceted cytokine in viral infections. *J Cell Physiol*. 2021;236(12):8000-8019.
43. Bulat V, Situm M, Azdajic MD, Likic R. Potential role of IL-17 blocking agents in the treatment of severe COVID-19? *Br J Clin Pharmacol*. 2021;87(3):1578-1581.
44. Megna M, Napolitano M, Fabbrocini G. May IL-17 have a role in COVID-19 infection? *Med Hypotheses*. 2020;140:109749.
45. Queiroz MAF, Neves PFM, Lima SS, et al. Cytokine profiles associated with acute COVID-19 and long COVID-19 syndrome. *Front Cell Infect Microbiol*. 2022;12:922422.
46. Lei L, Zhao C, Qin F, He ZY, Wang X, Zhong XN. Th17 cells and IL-17 promote the skin and lung inflammation and fibrosis process in a bleomycin-induced murine model of systemic sclerosis. *Clin Exp Rheumatol*. 2016;34 Suppl 100(5):14-22.
47. Lei L, He ZY, Zhao C, Sun XJ, Zhong XN. Elevated frequencies of CD4(+) IL-21(+) T, CD4(+) IL-21R(+) T and IL-21(+) Th17 cells, and increased levels of IL-21 in bleomycin-induced mice may be

- associated with dermal and pulmonary inflammation and fibrosis. *Int J Rheumatic Dis.* 2016;19(4):392-404.
48. Chen K, Eddens T, Trevejo-Nunez G, et al. IL-17 receptor signaling in the lung epithelium is required for mucosal chemokine gradients and pulmonary host defense against *K. pneumoniae*. *Cell Host Microbe.* 2016;20(5):596-605.
 49. Xia W, Bai J, Wu X, et al. Interleukin-17A promotes MUC5AC expression and goblet cell hyperplasia in nasal polyps via the Act1-mediated pathway. *PLoS ONE.* 2014;9(6):e98915.
 50. de Boer O, Li X, Teeling P, et al. Neutrophils, neutrophil extracellular traps and interleukin-17 associate with the organisation of thrombi in acute myocardial infarction. *Thromb Haemost.* 2013;109(2):290-297.
 51. Bouchnita A, Miossec P, Tosenberger A, Volpert V. Modeling of the effects of IL-17 and TNF- α on endothelial cells and thrombus growth. *C R Biol.* 2017;340(11-12):456-473.
 52. Ding P, Zhang S, Yu M, et al. IL-17A promotes the formation of deep vein thrombosis in a mouse model. *Int Immunopharmacol.* 2018;57:132-138.
 53. Sun J, Madan R, Karp CL, Braciale TJ. Effector T cells control lung inflammation during acute influenza virus infection by producing IL-10. *Nature Med.* 2009;15(3):277-284.
 54. Nelson CE, Foreman TW, Kauffman KD, et al. IL-10 suppresses T cell expansion while promoting tissue-resident memory cell formation during SARS-CoV-2 infection in rhesus macaques. *bioRxiv.* Preprint posted online September 15, 2022. 2022. doi:10.1101/2022.09.13.507852

SUPPORTING INFORMATION

Additional supporting information can be found online in the Supporting Information section at the end of this article.

How to cite this article: Zhang T, Magazine N, McGee MC, et al. Th2 and Th17-associated immunopathology following SARS-CoV-2 breakthrough infection in Spike-vaccinated ACE2-humanized mice. *J Med Virol.* 2024;96:e29408. doi:10.1002/jmv.29408